

Developmental Cell

Supplemental Information

**Cell Density Sensing Alters TGF- β Signaling
in a Cell-Type-Specific Manner,
Independent from Hippo Pathway Activation**

Flore Nallet-Staub, Xueqian Yin, Cristèle Gilbert, Véronique Marsaud, Saber Ben Mimoun, Delphine Javelaud, Edward B. Leof, and Alain Mauviel

SUPPLEMENTAL FIGURES

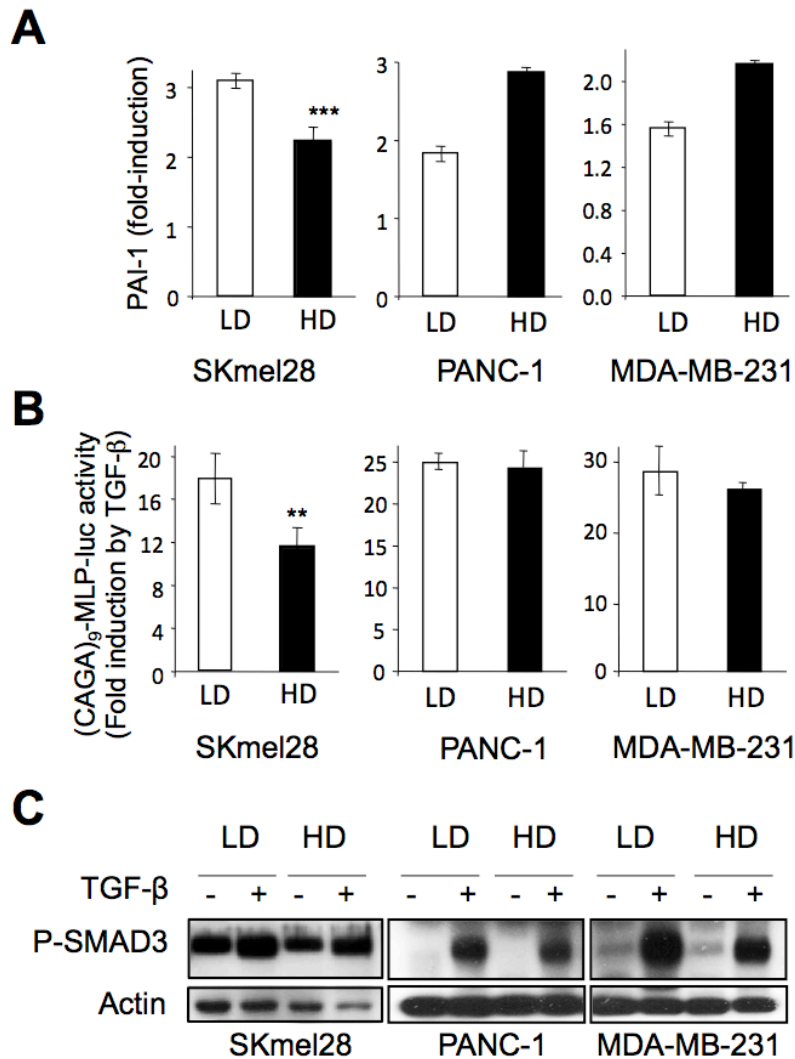


Figure S1. Impact of cell density on TGF-β signaling (related to Figure 1). SKmel28 melanoma cells, PANC-1 pancreatic and MDA-MB-231 breast carcinoma cells were grown in either low (LD) or high (HD) density conditions prior to TGF-β (5ng/ml) stimulation, as in Figure 1. **A.** Quantitative reverse transcriptase-PCR analysis of *PAI-1* expression after a 24h TGF-β treatment. Results are expressed as fold induction by TGF-β in each culture condition and are the mean±s.d. of two independent experiments, each measured in triplicate. **B.** Effect of TGF-β on SMAD3/4-specific transcription. Results are expressed as fold activation of transiently transfected (CAGA)₉-MLP-luc activity 18h after TGF-β addition to the cultures. Results are the mean±s.d. of two independent experiments, each performed with triplicate samples. **C.** Western analysis of P-SMAD3 levels without or with 30min TGF-β stimulation. Actin levels were measured as a control for the specificity of P-SMAD3 changes under each experimental condition. Results from one representative of several independent experiments are shown.

A

	% Nuclear SMAD3	% Nuclear TAZ
HaCaT - TGF- β	3 \pm 0.8	0.8 \pm 0.7
HaCaT + TGF- β	96.4 \pm 1.0	0.8 \pm 0.8
1205 - TGF- β	7.3 \pm 5.0	5.6 \pm 0.6
1205 + TGF- β	73.8 \pm 10	6.9 \pm 2.0
EpH4 - TGF- β	5.5 \pm 2.9	5.7 \pm 4.0
EpH4 + TGF- β	9.3 \pm 1.6	7.7 \pm 0.6

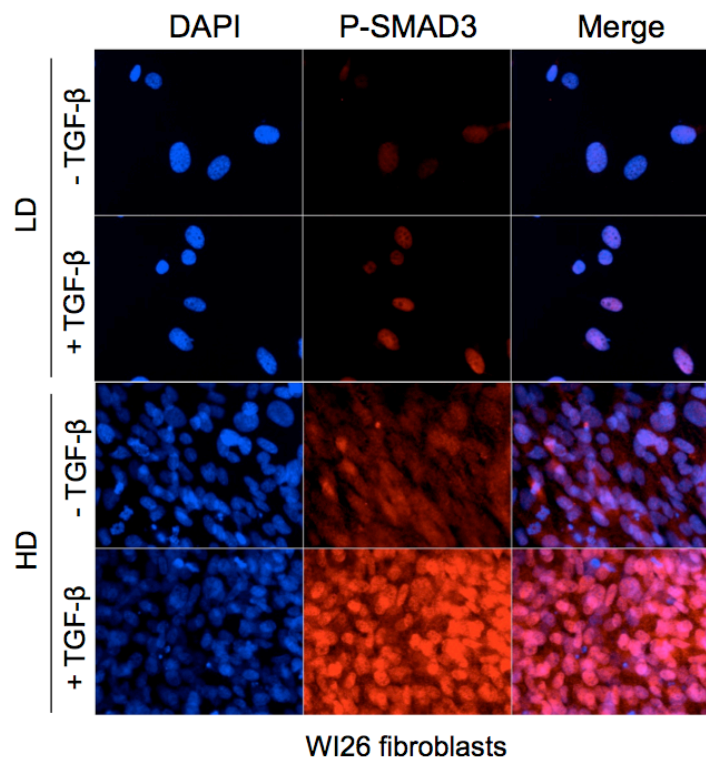
B

Figure S2. A. Quantitation of SMAD3 and TAZ nuclear localization in high density cultures of HaCaT, 1205Lu, and EpH4 cells in absence or presence of TGF- β (related to Figure 2). Results are the mean \pm s.e.m. of two independent measures by two distinct scientists using Image J software. Note the dramatic nuclear accumulation of SMAD3 upon TGF- β treatment in HaCaT and 1205Lu cells, not in EpH4, while TAZ remains essentially cytoplasmic in all cell lines.

B. High cell density does not prevent TGF- β -induced nuclear accumulation of P-SMAD3 in WI26 lung fibroblasts. Cells were grown on glass coverslips in either low (LD) or high (HD) density conditions prior to TGF- β (30min., 5ng/ml) stimulation, then subjected to immunofluorescent detection of P-SMAD3 (red). Nuclei (blue) were stained with DAPI.

Experiments were repeated several times with similar results. A representative experiment is shown. Note that nuclear accumulation of P-SMAD3 in response to TGF- β is stronger in dense vs. sparse fibroblast culture conditions, consistent with early observations on TGF- β -driven gene expression (see related references in the Introduction).

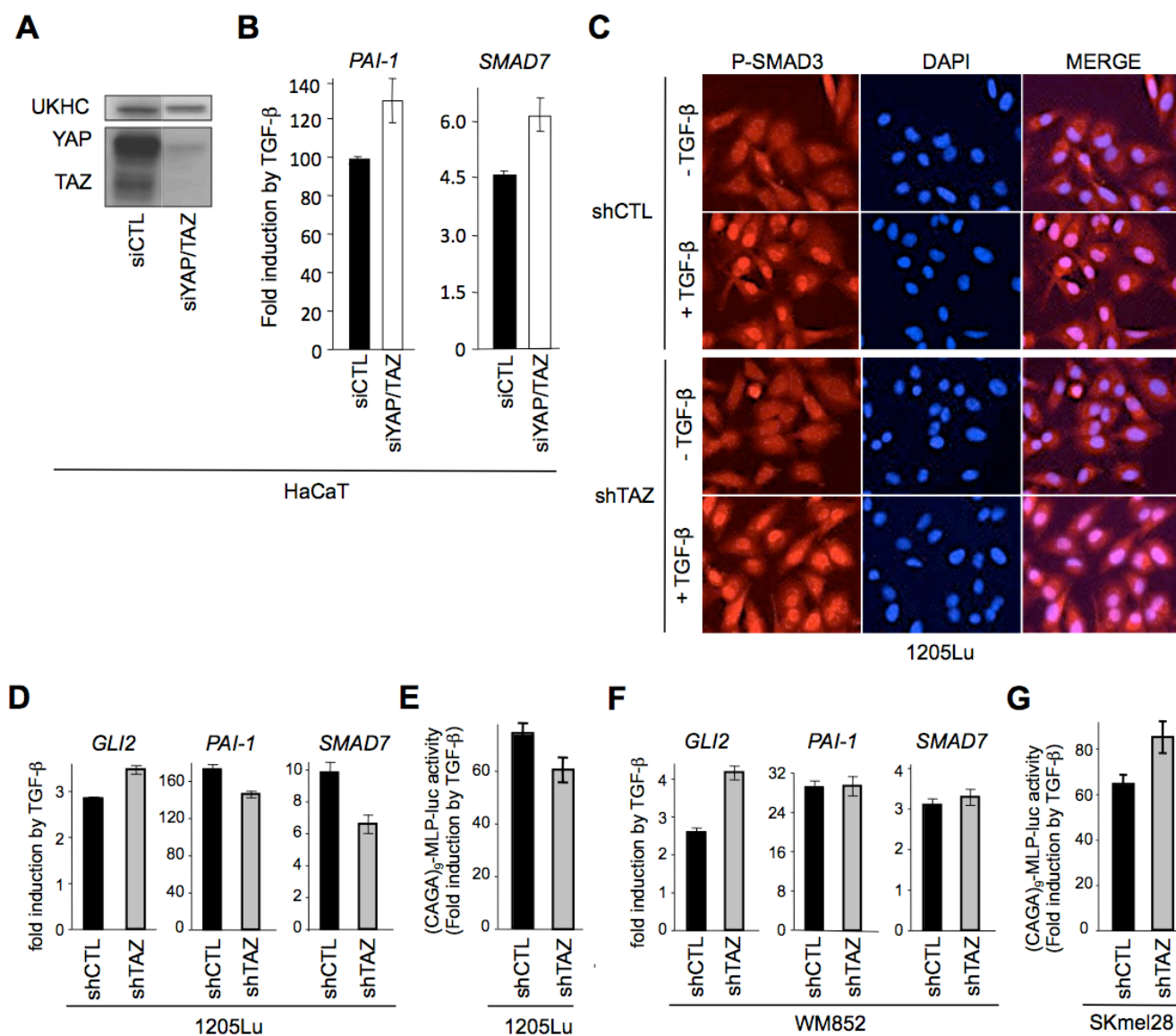


Figure S3. Altering cellular YAP/TAZ levels does not affect the extent of TGF- β responses (related to Figure 2). **A.** Western analysis of YAP and TAZ protein levels in siCTL- and siYAP+siTAZ-transfected HaCaT cells. **B.** Quantitative RT-PCR analysis of *PAI-1* (left) and *SMAD7* (right) transcript levels in siCTL- and siYAP/TAZ-transfected HaCaT cells after a 24h TGF- β stimulation. Results are expressed as fold induction by TGF- β under each culture condition. **C.** Immunofluorescent detection of P-SMAD3 in 1205Lu melanoma cells without (shCTL) or with stable knockdown of TAZ (shTAZ). Nuclei (blue) were stained with DAPI. **D.** Quantitative reverse transcriptase-PCR analysis of *GLI2*, *PAI-1*, and *SMAD7* expression in shCTL and shTAZ 1205Lu cells following a 24h TGF- β treatment. Results are expressed as fold induction by TGF- β in each culture condition and are the mean \pm s.d. from two independent experiments, each measured in triplicate. **E.** Effect of TGF- β on SMAD3/4-specific transcription in shCTL

and shTAZ 1205Lu cells. Results are expressed as fold activation of transiently transfected (CAGA)₉-MLP-luc activity 18h after TGF- β addition to the cultures. Results are the mean \pm s.d. of two independent experiments, each performed with triplicate samples. **F.** Quantitative reverse transcriptase-PCR analysis of GLI2, PAI-1, and SMAD7 expression in shCTL and shTAZ WM852 melanoma cells following a 24h TGF- β treatment. **G.** Effect of TGF- β on SMAD3/4-specific transcription in shCTL and shTAZ SKmel28 cells. Results are expressed as fold activation of transiently transfected (CAGA)₉-MLP-luc activity 18h after TGF- β addition to the cultures. Results for panels **F** and **G** reflect the mean \pm s.d. of two independent experiments, each performed with triplicate samples. Efficacy and specificity of TAZ (or YAP) knockdown was validated by Q-PCR and Western blotting (for details, see Nallet-Staub et al., *J. Invest. Dermatol.* 2014, Supplementary Fig. S2)

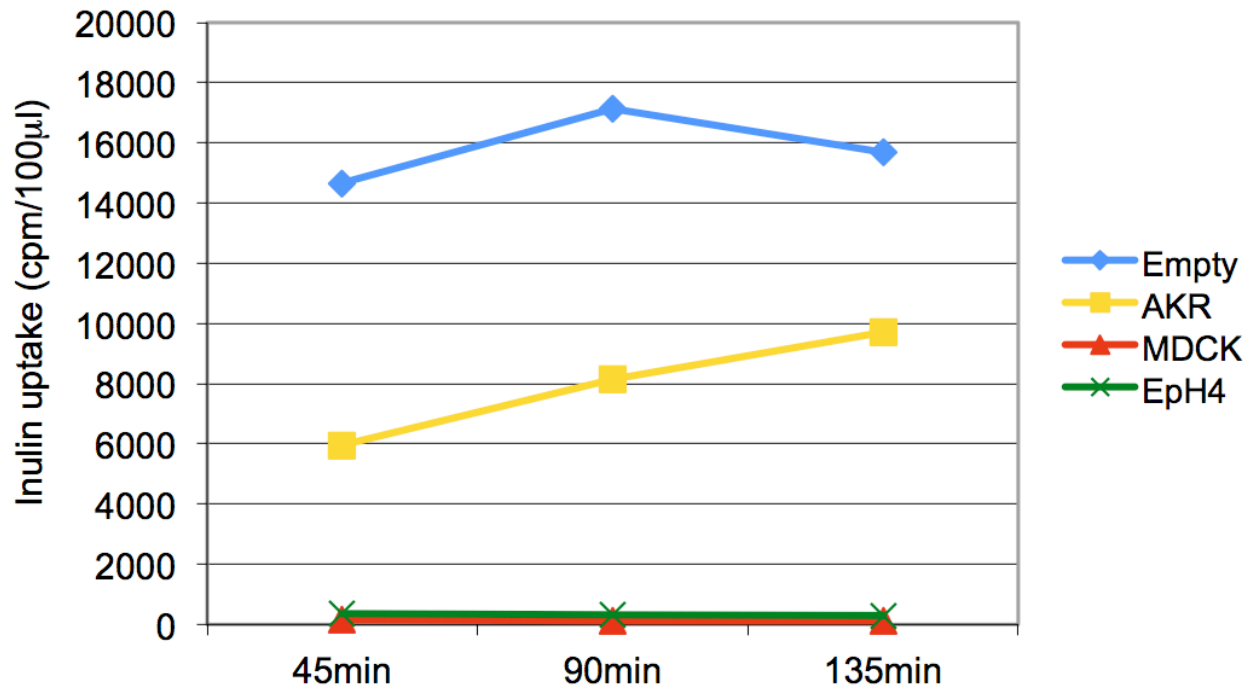


Figure S4. Inulin flux in confluent AKR-2B fibroblasts, EpH4, and MDCK cell Transwell cultures (related to Figure 3). Cells were grown to confluency in Transwells. Inulin flux from the apical to basal chambers was determined over time. Empty reflects inulin flux in the absence of plated cells. Note the absence of inulin flux in both EpH4 and MDCK cells.

Supplemental Experimental Procedures

Generation of cell-permeable TAT-Smad3 and Tat-Smad3P protein. Expression

plasmid construction: Full-length rat Smad3 cDNA was cloned as a *KpnI/XhoI* fragment into pTAT vector (Nagahara et al 1998) to generate pTAT-Smad3 as a His-tagged TAT-Smad3 fusion. **Protein induction and purification:** pTAT-Smad3 was transformed into BL21(DE3)pLysS competent *E.coli* (Life-Technologies). Positive colonies were selected by Ampicillin (Sigma-Aldrich) and induced by IPTG (Life-Technologies) at 37°C for 5h. The bacterial pellet was suspended in wash buffer (Na₂HPO₄ 50mM, NaCl 300mM pH 7.0) and processed by Lysozyme (Sigma-Aldrich) digestion and sonication prior to Talon resin (Clontech) purification. The column was washed with 25mM Imidazole/wash buffer and His-tagged TAT-Smad3 protein eluted by 150mM Imidazole/wash buffer. Concentration and purity of TAT-Smad3 was measured with a BCA protein assay kit (Thermo Scientific) and confirmed by Coomassie (Sigma-Aldrich) staining. ***In vitro* phosphorylation of TAT-Smad3:** AKR-2B cells were stimulated with TGF-β1 (10ng/ml) at 37°C for 30min then lysed in modified RIPA buffer (50mM Tris-HCl pH 7.4, 150mM NaCl, 0.25% Na-deoxycholate, 1% IGEPAL, CA-630, 1mM EDTA, 50mM NaF, 1mM Na₃VO₄, 1mM phenylmethylsulfonyl fluoride, and protease inhibitor cocktail (Roche). Phosphorylated/activated endogenous TβR1 was purified with a Catch and Release Reversible Immunoprecipitation System (Millipore). Briefly, 500μg total protein and 2.5μg TβR1 antibody (Santa-Cruz) were applied to the resins and the active form of TβRI was eluted in kit-provided non-denaturing buffer. 10μg of TAT-Smad3 was used as substrate for *in vitro* phosphorylation at 37°C for

30min in a reaction mix consisting of 50mM Tris-HCl, 10mM MgCl₂, 1mM DTT, 5μl of pTβR1 product, with or without 5μM ATP.

YAP and TAZ gene silencing

For transient gene silencing, HaCaT cells were transfected with two distinct siRNAs specifically targeting YAP or TAZ (Sigma-Aldrich human YAP or TAZ Mission siRNAs SASI_Hs01_00182403 and SASI_Hs01_00124479, respectively). The siRNA sequences were different from those from the shRNA lentiviral vectors. Sequence details may be found in (Nallet-Staub et al 2014). A non-targeting siRNA (Sigma- Aldrich Mission Universal Negative control siRNA #2) was used as control. For experiments requiring RNA or protein extraction, cells were seeded at 2×10^5 cells/well in 6-well plates and transfected 24h later in fresh medium containing 1% FCS with siRNA (150 ng/well) using 12 μl of HiPerfect reagent. Sample processing occurred 48h later. Stable TAZ knockdown in melanoma cell lines has been described previously (Nallet-Staub et al 2014).

Inulin assay

Inulin flux was measured by plating 5×10^4 cells/12-mm Transwell dish in 10% FBS/DMEM and allowing them to grow for 3 days. Details may be found in (Yin et al 2013).

Oligonucleotides for quantitative RT-PCR

Target	Forward	Reverse
human <i>GLI2</i>	ACCAACCAGAACAAGCAGAGC	ATGGCGACAGGGTTGACG
human <i>PAI-1</i>	GCTTTTGTGTGCCTGGTAGAAA	TGGCAGGCAGTACAAGAGTGA
human <i>GAPDH</i>	TGGGTGTGAACCATGAGAAGTATG	GGTGCAGGAGGCATTGCT
human or mouse <i>SMAD7</i>	TTTGCCTCGGACAGCTCAAT	ATTTTGTCTCCGCACCTTCTG
mouse <i>JunB</i>	AGGCAGCTACTTTTCGGGTCAGGG	CAGGGCTTTGACAAAACCGTC CGC
mouse <i>Ctgf</i>	GTGCCAGAATGCACACTG	CCCCGGTTACACTCCAAA
mouse <i>Hprt</i>	CAAGCTTGCTGGTGAAAAGGA	TGCGCTCATCTTAGGCTTTGTA

Western blotting (WB) and Immunofluorescence (IF) Antibodies

Specificity	Source	Notes
Actin	Sigma #A4700	WB 1:500
Akt	Cell Signaling Technology #9272	WB 1:1000
E-Cadherin	BD Biosciences #610181	WB 1:10000
HA	Cell Signaling Technology #3724 or Roche 12CA5#11666606001	IF 1:100 IF 1:500
Myc	Cell Signaling Technology #2278	IF 1:100
SMAD2/3	Santa Cruz Biotechnology #sc-8332	IF 1:200
SMAD3	Abcam ab28379	IF 1:200 WB 1:1000
p-SMAD3(pS423, pS425)	Leof laboratory, Mayo clinic	WB 1:50000
TAZ	Cell Signaling Technology #4883 or BD #560235	IF 1:200 WB 1:5000 IF 1:200
T β RI	Santa Cruz Biotechnology #sc-398	WB 1:500
T β RII	Santa Cruz Biotechnology #sc-220	WB 1:500
UKHC	Santa Cruz Biotechnology #sc-13356	WB 1:1000
YAP	Santa Cruz Biotechnology #sc-15407	WB 1:1000
Cy3 Donkey anti-Rabbit	Jackson ImmunoResearch Laboratories Inc. 711-165-152	IF 1:250
488 Goat Anti-Mouse	Life Technologies A-11001	IF 1:250

SUPPLEMENTAL REFERENCES

Nagahara H, Vocero-Akbani AM, Snyder EL, Ho A, Latham DG, Lissy NA *et al* (1998). Transduction of full-length TAT fusion proteins into mammalian cells: TAT-p27Kip1 induces cell migration. *Nature Med.* 4, 1449-1452.

Nallet-Staub F, Marsaud V, Li L, Gilbert C, Dodier S, Bataille V *et al* (2014). Pro-invasive activity of the Hippo pathway effectors YAP and TAZ in cutaneous melanoma. *J. Invest. Dermatol.* 134, 123-132.

Yin X, Murphy SJ, Wilkes MC, Ji Y, Leof EB (2013). Retromer maintains basolateral distribution of the type II TGF-beta receptor via the recycling endosome. *Mol. Biol. Cell* 24, 2285-2298.